Original Article

MOLECULAR METABOLISM

The absence of hepatic glucose-6 phosphatase/ChREBP couple is incompatible with survival in mice

Fabienne Rajas [1,*], Renaud Dentin [2], Alexane Cannella Miliano [1], Marine Silva [1], Margaux Raffin [1], Françoise Levavasseur [2], Amandine Gautier-Stein [1], Catherine Postic [2], Gilles Mithieux [1]

ABSTRACT

Objective: Glucose production in the blood requires the expression of glucose-6 phosphatase (G6Pase), a key enzyme that allows glucose-6 phosphate (G6P) hydrolysis into free glucose and inorganic phosphate. We previously reported that the hepatic suppression of G6Pase leads to G6P accumulation and to metabolic reprogramming in hepatocytes from liver G6Pase-deficient mice (L.G6pc$^{-/-}$). Interestingly, the activity of the transcription factor carbohydrate response element-binding protein (ChREBP), central for *de novo* lipid synthesis, is markedly activated in L.G6pc$^{-/-}$ mice, which consequently rapidly develop NAFLD-like pathology. In the current work, we assessed whether a selective deletion of ChREBP could prevent hepatic lipid accumulation and NAFLD initiation in L.G6pc$^{-/-}$ mice.

Methods: We generated liver-specific ChREBP (L.Chrebp$^{-/-}$)- and/or G6Pase (L.G6pc$^{-/-}$)-deficient mice using a Cre-lox strategy in B6.SA^{CreERT2} mice. Mice were fed a standard chow diet or a high-fat diet for 10 days. Markers of hepatic metabolism and cellular stress were analysed in the liver of control, L. G6pc$^{-/-}$, L. Chrebp$^{-/-}$ and double knockout (i.e., L.G6pc$^{-/-}$.Chrebp$^{-/-}$) mice.

Results: We observed that there was a dramatic decrease in lipid accumulation in the liver of L.G6pc$^{-/-}$.Chrebp$^{-/-}$ mice. At the mechanistic level, elevated G6P concentrations caused by lack of G6Pase are rerouted towards glycogen synthesis. Importantly, this exacerbated glycogen accumulation, leading to hepatic water retention and aggravated hepatomegaly. This caused animal distress and hepatocyte damage, characterised by ballooning and moderate fibrosis, paralleled with acute endoplasmic reticulum stress.

Conclusions: Our study reveals the crucial role of the ChREBP-G6Pase duo in the regulation of G6P-regulated pathways in the liver.

Keywords Glucose production; Glucose-6 phosphate; Glycaemia; Glycogen storage disease type 1; Non-alcoholic fatty liver disease; Type 2 diabetes

1. INTRODUCTION

Glucose production, from both glycogenolysis and gluconeogenesis, requires the expression of glucose-6 phosphatase (G6Pase) that allows the hydrolysis of glucose-6 phosphate (G6P) into free glucose and inorganic phosphate. This enzyme is specifically expressed in the liver, kidney and intestine, which explains the unique ability of these organs to produce glucose in the bloodstream [1–3]. During food assimilation, the liver stores glucose in the form of glycogen that can then be rapidly mobilised to produce glucose from the very first hours of fasting [2–4]. Thus, at the beginning of the post-absorptive period, the liver accounts for at least 80% of endogenous glucose production (EGP) [2,3]. When fasting is prolonged, glucose is mainly produced from non-carbohydrate precursors *via* gluconeogenesis. After the depletion of liver glycogen stores, the kidneys and intestine, the two other glucose-producing organs, increasingly contribute to glucose production, mainly from glutamine, while hepatic glucose production is reduced [2,3].

Another crucial function of the liver is the coordination of body lipid metabolism, especially *via* the remodelling of captured lipoproteins and the delivery of very low-density lipoproteins (VLDL) to the blood. The liver is also the principal organ responsible for the conversion of excess carbohydrates into fat *via* the activation of the *de novo* lipogenesis pathway [5]. In metabolic diseases, such as obesity or type 2 diabetes, impaired glucose metabolism in the liver is associated with an excess of triglyceride (TG) content, a hallmark of non-alcoholic fatty liver disease (NAFLD) [5,6]. In this context, the net accumulation of lipid droplets within the liver is associated with 1) an increase of fatty acid esterification of free fatty acids, 2) an activation of *de novo* lipogenesis, 3) a decrease of fatty acid oxidation and 4) a decrease of VLDL export

[1]Université Claude Bernard Lyon 1, Université de Lyon, INSERM UMR-1213, Lyon, France [2]Université de Paris, Institut Cochin, CNRS, INSERM, Paris, France

*Corresponding author. Inserm UMR-1213 "Nutrition, Diabetes and the Brain", Université Lyon 1 Laennec, 7 rue Guillaume Paradin, 69372 Lyon cedex 08, France. E-mail: fabienne.rajas@univ-lyon1.fr (F. Rajas).

Abbreviations: Aspartate aminotransferase, AST; alanine aminotransferase, ALT; carbohydrate response element-binding protein, ChREBP; endogenous glucose production, EGP; free fatty acid, FFA; glucose-6 phosphatase, G6Pase; glucose-6 phosphate, G6P; non-alcoholic fatty liver disease, NAFLD; non-esterified fatty acid, NEFA; triglycerides, TG; very low-density lipoproteins, VLDL; wild-type, WT

Received August 13, 2020 • Revision received October 27, 2020 • Accepted October 28, 2020 • Available online 31 October 2020

https://doi.org/10.1016/j.molmet.2020.101108

[7,8]. Under pathophysiological conditions characterised by excess of carbohydrates, the activation of *de novo* lipogenesis is mediated by the carbohydrate response element-binding protein (ChREBP), which co-ordinates postprandial hepatic glycolysis and lipogenesis [9,10]. This transcriptional factor positively regulates the expression of numerous glycolytic/lipogenic genes in response to high glucose or G6P concentration. Interestingly, global or liver-specific ChREBP deficiency in diabetic obese *ob/ob* mice or in mice fed a high-carbohydrate diet significantly reduces liver steatosis by decreasing lipogenic rates [11–13]. Moreover, plasma TG and free fatty acid (FFA) levels are lower in Chrebp$^{-/-}$ mice than in wild-type (WT) mice. These results suggest that selectively suppressing ChREBP activity in the liver could prevent NAFLD and hypertriglyceridaemia. While ChREBP inhibition efficiently reduces lipogenesis, its impact on glucose homeostasis needs to be clarified.

We previously reported that G6Pase suppression in the liver of mice (L.G6pc$^{-/-}$) leads to G6P accumulation and to metabolic reprogramming in hepatocytes [14–16]. ChREBP activity and gene expression are also markedly activated in the livers of L.G6pc$^{-/-}$ mice, resulting in the rapid development of an NAFLD-like phenotype [14,15,17]. We recently showed that lipids play a crucial role in hepatic injury and tumourigenesis development, both being prevented by lipid-lowering treatments [18]. In the current study, we address whether the suppression of ChREBP in the livers of L.G6pc$^{-/-}$ mice can prevent the accumulation of lipids and the initiation of NAFLD, as well as liver damage. Our results reveal that the combined deficiency in G6Pase and ChREBP results in severe liver damage and animal distress, highlighting the vital role of the ChREBP-G6Pase couple in maintaining liver homeostasis.

2. METHODS

2.1. Animals and diets

The deficiency in hepatic G6PC and/or ChREBP was obtained by the deletion of *G6pc1* exon 3 and/or *Mlxipl* exons 9–15, specifically in the liver due to an inducible CRE/lox strategy in mice. Mouse genotypes were determined using polymerase chain reaction (PCR, list of primer sequences in Table S1) from genomic DNA extracted in PCR direct lysis buffer (Euromedex). Adult (6–8 weeks) male B6.G6pc1$^{lox/lox}$.Chrebp$^{lox/lox}$.SA$^{wt/wt}$, B6.G6pc1$^{lox/lox}$.SA$^{CreERT2/wt}$, B6.Chrebp$^{lox/lox}$.SA$^{CreERT2/wt}$ and B6.G6pc1$^{lox/lox}$.Chrebp$^{lox/lox}$.SA$^{CreERT2/wt}$ mice received 0.2 mg of tamoxifen/day for 5 consecutive days to generate control (n = 8), L.G6pc$^{-/-}$ (n = 6), L.Chrebp$^{-/-}$ (n = 7) and L.G6pc$^{-/-}$.Chrebp$^{-/-}$ (n = 8) mice, respectively. The control mice were littermates of B6.G6pc$^{lox/lox}$.Chrebp$^{lox/lox}$.SA$^{CreERT2/wt}$ mice. After tamoxifen treatment, mice were either fed a chow diet (3.1% fat, 16.1% proteins, 60% starch carbohydrates, Safe) or a high-fat (HF) diet (35% fat, 20% protein, 35% starch carbohydrates, supplied by INRAE, Jouy-en-Josas). Animals were housed in the animal facility of University Lyon 1 in groups of 3–5 mice, in an enriched environment at 22–23 °C, with a light/darkness cycle (7 AM/7 PM). Mice had free access to water and facilitated access to food in the cage. All the procedures were performed in accordance with the principles and guidelines established by the European Convention for the Protection of Laboratory Animals. All conditions and experiments were approved by the University Lyon I animal ethics committee and the French Ministry of National Education, Higher Education and Research (Permit Apafis number: 12786-2017122020025366v1). Mice were killed 10 days after tamoxifen treatment, in the fed state at 10.00 AM. Livers were rapidly removed and frozen using tongs previously chilled in liquid nitrogen.

2.2. Histological analysis

A piece of fresh liver (of the largest lobe) was fixed in 10% formalin for 48 h, followed embedding in paraffin. Sections (4-μm-thick) were stained with haematoxylin and eosin (H&E) or Masson's trichrome by the "CiQLe" platform (University Lyon 1). The slides were examined under a Coolscope microscope (Nikon).

2.3. Analytical analyses

Blood was withdrawn by submandibular bleeding using a lancet and collected into ethylenediaminetetraacetic acid (EDTA) tubes. Plasma was obtained after centrifugation of blood for 10 min at 3,000 *g* at 4 °C. Blood glucose was measured with an Accu-Check Go glucometer (Roche Diagnostic). Plasma TG, cholesterol and non-esterified fatty acid (NEFA) were determined with colorimetric kits (DiaSys). Aspartate aminotransferase (AST)/alanine aminotransferase (ALT) activities were determined in plasma by a colorimetric activity kit (Abcam). The mouse enzyme-linked immunosorbent assay (ELISA) kit (BioVendor) was used to measure plasma FGF21. Hepatic glycogen and TG measurements were carried out in homogenates obtained by disruption of 50–100 mg of frozen livers with the FastPrep® instrument (MP Biomedicals). Hepatic glycogen was extracted by the Keppler and Decker method after glycogen hydrolysis; the glucose released was then measured [19]. Liver TGs were extracted using the Folch extraction procedure and measured with a colorimetric kit (DiaSys) as previously described [18].

2.4. Gene expression analysis by reverse transcription quantitative PCR (RT-qPCR)

Total RNAs were extracted from frozen livers according to the Trizol protocol (Invitrogen Life Technology). cDNA was generated from 500 ng of RNA using Quantities' Reverse Transcription Kit (Qiagen). PCR was performed using SSO Advanced Universal SYBR green Supermix (Bio-Rad) and expressed in 2-DDCT value using the mean values from control mice as normalisation. Amplifications were performed using a CFX Connect Real-Time system (Bio-Rad), followed by a melt curve analysis. The mouse ribosomal protein L19 (Rpl19) or L32 (Rpl32) were used as reference. Data were analysed using the Bio-Rad CFX manager software (Bio-Rad). Primer sequences are described in Table S1.

2.5. Western blot analysis

A piece of 100 mg of frozen liver was homogenised and disrupted in lysis buffer supplemented with protein and phosphatase inhibitor cocktail using a FastPrep® instrument (MP Biomedicals). Proteins were assayed with Pierce™ BCA Protein Assay Kit (Thermo Scientific). An aliquot of 30 μg of proteins (or 60 μg of proteins when it is mentioned in figure legend) was separated onto stain-free polyacrylamide gels (Bio-Rad) and transferred onto a polyvinylidene difluoride (PVDF) membrane. Antibody references and dilutions used for western blot analyses are cited in Table S2. The visualisation and quantification of the proteins were performed using Bio-Rad Chem-iDocTM Touch Imaging System. The normalisation of blots was performed by measuring the total band density (= total amount of proteins) of each lane using the stained-free imaging technology developed by Bio-Rad [20]. The background was subtracted from the sum of density of all bands in each lane.

2.6. Statistics

The results are expressed as mean ± s.e.m. Groups were compared using two-way analysis of variance (ANOVA) followed Tukey's multiple comparison post hoc test. Statistical analysis was performed using

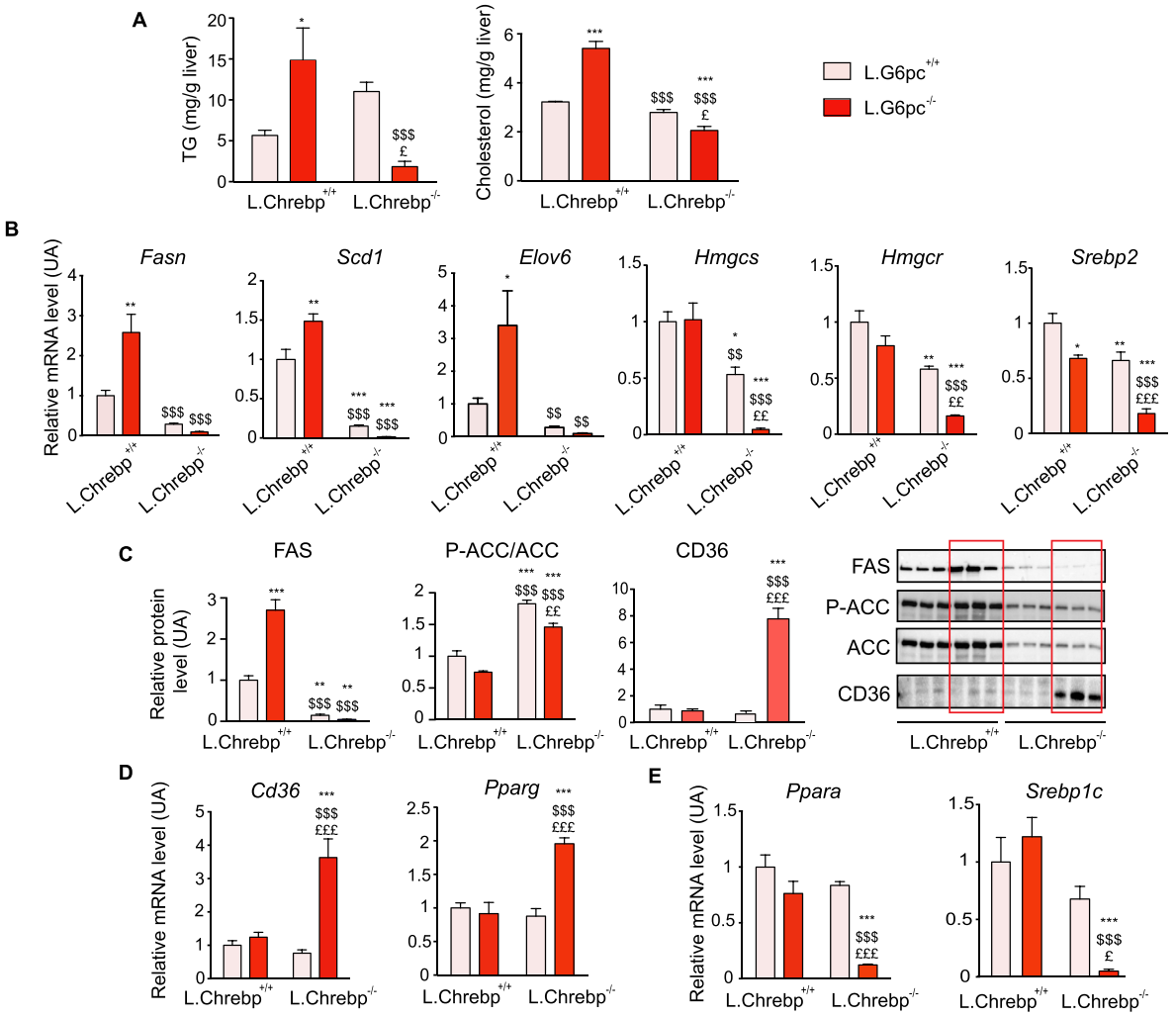

Figure 1: The loss of hepatic ChREBP prevents non-alcoholic fatty liver disease in L.G6pc$^{-/-}$ mice. Control and L.Chrebp$^{-/-}$ mice (pink bars) and L.G6pc$^{-/-}$ and L.G6pc$^{-/-}$.Chrebp$^{-/-}$ mice (red bars) were fed a standard during 10 days after tamoxifen treatment. (**A)** Hepatic TG and cholesterol content (n = 6–8/group); (**B, D and E)** Relative mRNA expression of genes involved in lipid metabolism and lipid transport (n = 5–6/group). (**C)** Relative expression of FAS, CD36 and phosphorylated (P-ACC) or total ACC protein analysed by western blot. Representative images of blots (n = 3) and quantification graphs (6–8 samples/group) are shown. The quantification of FAS and CD36 was performed relatively to total amount of proteins using stained-free imaging technology (See Figure S5). The quantification of P-ACC was expressed relatively to the total ACC protein quantity. Data are expressed as mean ± s.e.m. *p < 0.05, **p < 0.01 and ***p < 0.001 indicate significance compared to control mice; $^{\$}$p < 0.05, $^{\$\$}$p < 0.01 and $^{\$\$\$}$p < 0.001 indicate significance compared to L.G6pc$^{-/-}$ mice; $^{£}$p < 0.05, $^{££}$p < 0.01 and $^{£££}$p < 0.001 indicates significance compared to L.Chrebp$^{-/-}$ mice. See also Figure S2.

GraphPad Prism v6 software. Differences were considered to be statistically significant at p value < 0.05.

3. RESULTS

3.1. Loss of hepatic ChREBP markedly decreases lipid accumulation in liver of L.G6pc $^{-/-}$ mice

To evaluate the specific contribution of ChREBP to the fatty liver phenotype of L.G6pc$^{-/-}$ mice, knockout mice deficient for both ChREBP and G6Pase were generated (L.G6pc$^{-/-}$ Chrebp$^{-/-}$ mice). Targeted deletion of *Mlxipl* exons 9–15 was achieved in the liver of adult L.G6pc$^{-/-}$ mice by using the inducible CRE-lox strategy we previously used to obtain the deletion of *G6pc1* exon 3 [15]. B6.G6pc1$^{lox/lox}$.Chrebp$^{lox/lox}$.SA$^{wt/wt}$, B6.G6pc1$^{lox/lox}$.SA$^{CreERT2/wt}$, B6.Chrebp$^{lox/lox}$.SA$^{CreERT2/wt}$ and B6.G6pc1$^{lox/lox}$.Chrebp$^{lox/lox}$.SA$^{CreERT2/wt}$ mice were treated by tamoxifen at 6–8 weeks of age to obtain control, L.G6pc$^{-/-}$, L.Chrebp$^{-/-}$ and L.G6pc$^{-/-}$.Chrebp$^{-/-}$mice, respectively. The restricted loss of *Mlxipl* and *G6pc1* expression in the liver of L.G6pc$^{-/-}$.Chrebp$^{-/-}$ mice was confirmed by RT-qPCR and G6Pase enzymatic activity, respectively (Figure S1).

Ten days post-deletion, L.G6pc$^{-/-}$ mice developed a moderate steatosis compared to WT mice, and the loss of hepatic ChREBP resulted in a striking decrease in TG content in the livers of L.G6pc$^{-/-}$.Chrebp$^{-/-}$ compared to L.G6pc$^{-/-}$ mice (Figure 1A). Hepatic TG levels in L.G6pc$^{-/-}$.Chrebp$^{-/-}$ mice were even significantly lower than that in control mice (Figure 1A). Hepatic cholesterol content was also decreased in L.G6pc$^{-/-}$.Chrebp$^{-/-}$ mice compared to that in L.G6pc$^{-/-}$ mice as well as control and L.Chrebp$^{-/-}$ mice (Figure 1A). This was linked to a marked decreased in the expression of *Fasn, Scd1* and *Elov6* lipogenic genes as well as of genes involved in cholesterol synthesis (*Hmgcs, Hmgcr, Srebp2*) in the livers of double knockout mice compared to

both L.G6pc$^{-/-}$ and control mice (Figure 1B). The quantity of FAS was markedly decreased in the livers of double knockout mice (Figure 1C). In addition to the decrease in ACC protein content, the relative phosphorylation of ACC was increased in L.G6pc$^{-/-}$.Chrebp$^{-/-}$ and L.Chrebp$^{-/-}$ livers, suggesting a decrease in its activity (Figure 1C). Surprisingly, hepatic TG and cholesterol content in L.Chrebp$^{-/-}$ mice were similar as that in control mice, whereas lipogenic gene expression was lower (Figure 1). Interestingly, the expression of *Cd36*, coding for a trafficking protein (FAT/CD36) known to enhance fatty acid uptake [21], was increased in L.G6pc$^{-/-}$.Chrebp$^{-/-}$ livers, compared to both L.G6pc$^{-/-}$ and controls (Figure 1C—D). *Cd36* is a target gene of PPARγ, which was also increased in L.G6pc$^{-/-}$.Chrebp$^{-/-}$ livers (Figure 1D). These data suggest a liver adaptation promoted by the low level of lipids to increase fatty acid uptake. Moreover, it should be noted that the expression of transcription factors linked to lipid metabolism, such as Sterol Element Binding Element Protein-1c (encoded by *Srebp1c*) and *Ppara* were strongly decreased in double knockout livers, compared to both control and L. Chrebp$^{-/-}$ livers (Figure 1E). Regarding the plasma profile, TG and cholesterol levels were higher in L.G6pc$^{-/-}$.Chrebp$^{-/-}$ mice compared to control and L.G6pc$^{-/-}$ mice, while NEFA levels were unchanged (Table 1).

Because L.G6pc$^{-/-}$.Chrebp$^{-/-}$ mice showed a lower body weight than L.G6pc$^{-/-}$ and control mice (Table 1) and general illnessand distress about 9—10 days after tamoxifen treatment, mice of each genotype were fed a HF diet to increase food calorie intake. No simple carbohydrates were added to the diet to moderate G6P production and glycogen accumulation and try to prevent the deleterious effects observed in L.G6pc$^{-/-}$ mice fed a high-fat/high-sucrose diet [14]. Despite higher fat intake, L.G6pc$^{-/-}$.Chrebp$^{-/-}$ mice did not accumulate hepatic TGs, while control, L.G6pc$^{-/-}$ and L.Chrebp$^{-/-}$ mice developed a marked steatosis (characterised by [TG] over 40 mg/g liver) (Figure S2A). This was associated with a decrease in *de novo* lipogenesis gene expression (Figure S2B). As previously observed (Figure 1A), hepatic cholesterol content in livers of L.G6pc$^{-/-}$.Chrebp$^{-/-}$ mice was similar to that in control and L.Chrebp$^{-/-}$ mice, while L.G6pc$^{-/-}$ mice accumulated higher hepatic levels of cholesterol (Figure S2A). Despite elevated hepatic *Cd36* expression in L.G6pc$^{-/-}$.Chrebp$^{-/-}$ mice fed a HF diet (Figure S2B), plasmatic TG, cholesterol and NEFA levels remained elevated compared to control mice (Table S3). Dyslipidaemia was even more pronounced than in L.G6pc$^{-/-}$ mice (Table S3). This was associated with a low body weight and the absence of adipose tissue in double knockout mice (Table S3). Interestingly, L.Chrebp$^{-/-}$ mice fed an HF diet had comparable plasmatic TGs and cholesterol concentrations as that in control mice, suggesting little impact of ChREBP deletion under these conditions (Table S3).

Altogether, these data reveal the importance of ChREBP in the fatty liver phenotype of L.G6pc$^{-/-}$ mice.

Table 1 — Body weight and plasma parameters of control, L.G6pc$^{-/-}$, L.Chrebp$^{-/-}$ and L.G6pc$^{-/-}$.Chrebp$^{-/-}$ mice.

	control mice (n = 8)	L.G6pc$^{-/-}$ mice (n = 6)	L.Chrebp$^{-/-}$ mice (n = 7)	L. G6pc$^{-/-}$.Chrebp$^{-/-}$ mice (n = 8)
Body weight (g)	27.8 ± 1.3	26.7 ± 0.8	23.9 ± 1.1	20.7 ± 0.5$^{***,\$}$
TG (g/L)	1.41 ± 0.06	1.26 ± 0.09	1.56 ± 0.22	1.96 ± 0 .16$^{*,\$\$}$
Cholesterol (g/L)	1.19 ± 0.08	1.23 ± 0.14	1.11 ± 0.08	3.32 ± 0.13$^{*,\$\$}$
NEFA (mg/dL)	28.07 ± 2.84	25.64 ± 1.98	20.95 ± 1.56	23.08 ± 1.34
Glucose (mg/dL)	162.3 ± 7.1	141.7 ± 13.0	179.6 ± 5.6	103.5 ± 7.5$^{***,\$}$

The results are expressed as mean ± s.e.m. A one-way ANOVA followed by Tukey's post hoc test was performed as a statistical analysis. *p < 0.05, **p < 0.01 and ***p < 0.001 versus WT mice. $^{\$}$p < 0.05 and $^{\$\$}$p < 0.01 versus L.G6pc$^{-/-}$ mice; n = number of samples.

3.2. Aggravation of glycogen storage disease by blocking lipid synthesis in L.G6pc$^{-/-}$ mice

As mentioned above, deletion of ChREBP in liver of L.G6pc$^{-/-}$ mice (L.G6pc$^{-/-}$.Chrebp$^{-/-}$ mice) resulted in major animal distress that required premature stopping of the experiments. L.G6pc$^{-/-}$.Chrebp$^{-/-}$ mice exhibited larger and clearer livers than L.G6pc$^{-/-}$ mice (Figure 2A). This light translucent colour suggested massive water accumulation in the liver, which was confirmed by the observation that protein concentration per gram of liver was much lower than that in control livers (Figure 2B). The aggravation of hepatomegaly was due to a massive accumulation of glycogen (Figure 2C); the hydrophilicity of glycogen likely explains the hepatic retention of water. While G6P concentrations were elevated in livers of L.G6pc$^{-/-}$.Chrebp$^{-/-}$ mice compared to controls, they were not further increased when compared to L.G6pc$^{-/-}$ livers. In contrast, glucose levels were markedly reduced in L.G6pc$^{-/-}$ and L.G6pc$^{-/-}$.Chrebp$^{-/-}$ mice compared to that in controls (Figure 2C). Similar observations were obtained when L.G6pc$^{-/-}$.Chrebp$^{-/-}$ mice were fed a HF diet (Figure S3, panel A). This phenotype was only observed in double knockout mice. Indeed, G6P and glycogen concentrations, as well as glucose levels, were minimally affected in the livers of L.Chrebp$^{-/-}$ mice compared to that in controls, with an only discrete impact on liver weight (Figure 2C and Figure S3). As expected, the expression of ChREBP targets involved in glycolysis (*Lpk* and *Gapdh*) or in the pentose phosphate pathway (PPP) (glucose-6 phosphate dehydrogenase; *G6pdh*) was drastically decreased in the absence of ChREBP (Figure 2D), suggesting that ChREBP loss leads to a blockade of all G6P-driven pathways, including glycolysis, PPP and *de novo* lipogenesis, with the exception of the glycogen synthesis pathway (the latter not involving ChREBP).

Altogether, our results suggest that the combined loss of G6Pase and ChREBP leads to the rerouting of G6P exclusively toward glycogen synthesis. This results in a marked increase in glycogen concentrations in L.G6pc$^{-/-}$·Chrebp$^{-/-}$ hepatocytes, which in turn caused water retention and hepatomegaly in the absence of lipid accumulation.

3.3. Loss of hepatic ChREBP and G6Pase leads to severe hepatic damages

To investigate the illness and distress of L.G6pc$^{-/-}$.Chrebp$^{-/-}$ mice and better understand the impact of this double deletion, we analysed hepatic functions and liver histology. L.G6pc$^{-/-}$.Chrebp$^{-/-}$ mice exhibited a dramatic increase in plasma transaminase levels (AST and ALT), especially ALT levels, compared to control or L.G6pc$^{-/-}$ mice, suggesting severe liver damage (Figure 3A). In line with this observation, plasma albumin concentrations were lower in L.G6pc$^{-/-}$.Chrebp$^{-/-}$ mice, confirming a decrease in one of the main hepatic function (Figure 3B). Moreover, L.G6pc$^{-/-}$.Chrebp$^{-/-}$ mice had lower blood glucose concentrations than L.G6pc$^{-/-}$ and control mice (Table 1), even when challenged on HF diet (Table S3). At the histologic level, G6pc$^{-/-}$.Chrebp$^{-/-}$ hepatocytes were enlarged, clear

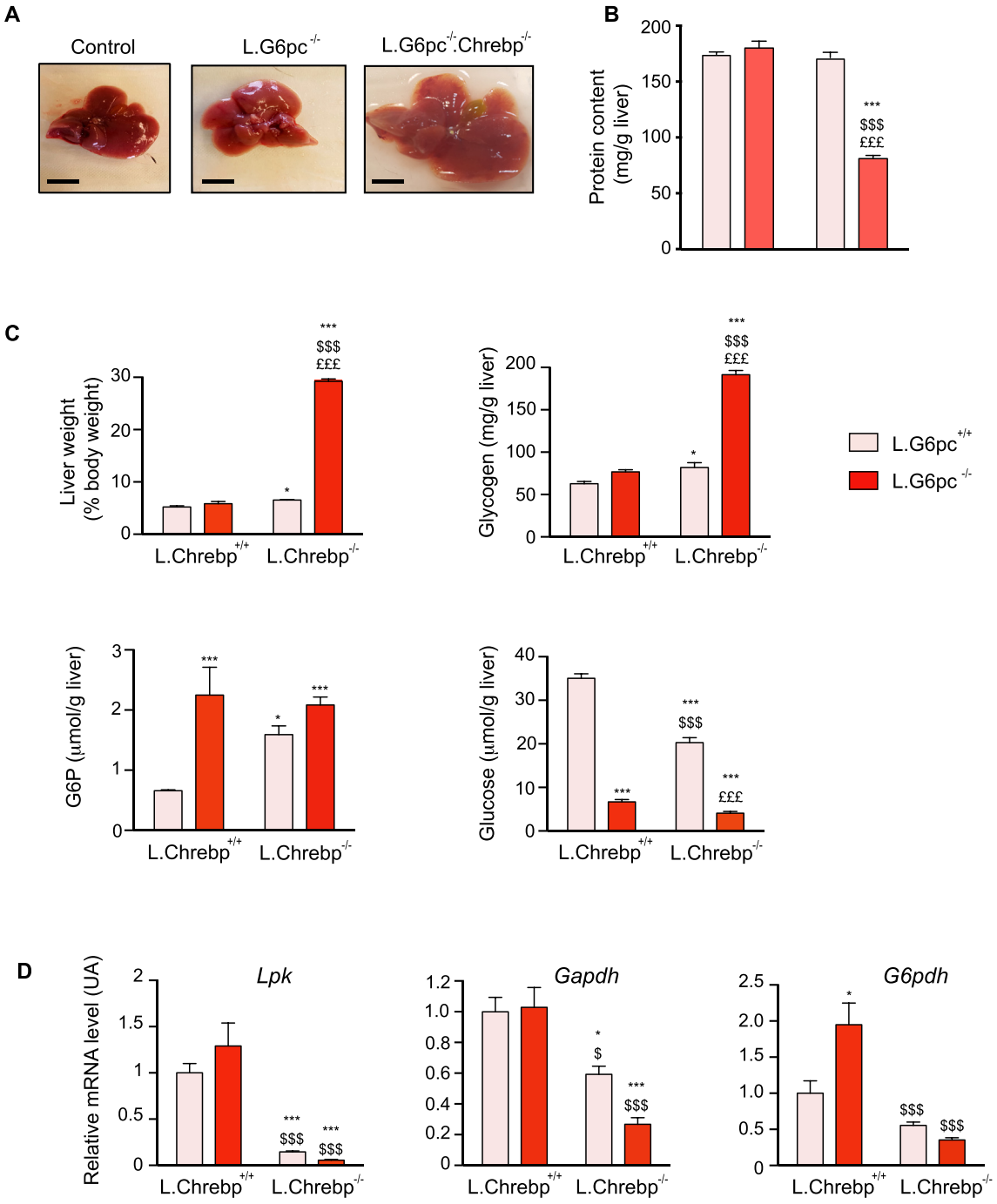

Figure 2: The loss of ChREBP in L.G6pc$^{-/-}$ livers aggravates hepatomegaly and leads to massive glycogen accumulation. Control and L.Chrebp$^{-/-}$ mice (pink bars) and L.G6pc$^{-/-}$ and L.G6pc$^{-/-}$.Chrebp$^{-/-}$ mice (red bars) were fed a standard diet during 10 days after tamoxifen treatment. **(A)** Representative pictures of livers; bars represent 1 cm; no photo available of the livers of the L.Chrebp$^{-/-}$ mice, which were very similar in appearance and colour to those of the control mice. **(B)** Protein content of the liver (n = 6–7/group). **(C)** Liver weight and hepatic glycogen, G6P and glucose content (n = 6–8/group). **(D)** Relative mRNA expression of genes involved in glycolysis (*Lpk* and *Gapdh*) and the pentose phosphate pathway (*G6pdh*) (n = 5–6/group). Data are expressed as mean ± s.e.m. *p < 0.05, **p < 0.01, ***p < 0.001 indicates significance compared to control mice; $^{\$}$p < 0.05, $^{\$\$}$p < 0.01, $^{\$\$\$}$p < 0.001 indicates significance compared to L.G6pc$^{-/-}$ mice; $^{£}$p < 0.05, $^{££}$p < 0.01 and $^{£££}$p < 0.001 indicates significance compared to L.Chrebp$^{-/-}$ mice. See also Figure S3.

and with signs of ballooning, compared to control, G6pc$^{-/-}$ and Chrebp$^{-/-}$ hepatocytes. Strikingly, no sign of inflammation could be histologically observed in L.G6pc$^{-/-}$.Chrebp$^{-/-}$ livers (Figure 3C). In the liver, the analysis of the expression of different inflammatory markers suggested a discrete inflammation state characterised by increased expression in MCP1 (monocyte chemoattractant protein 1) (Figure 3D) in double knockout mice compared control and L.G6pc$^{-/-}$ mice. At the mRNA levels, the expression of *Il6* (coding for interleukin 6) was also slightly increased in double knockout mice (Figure 3D). Il6 levels were also significantly increased in the plasma of double

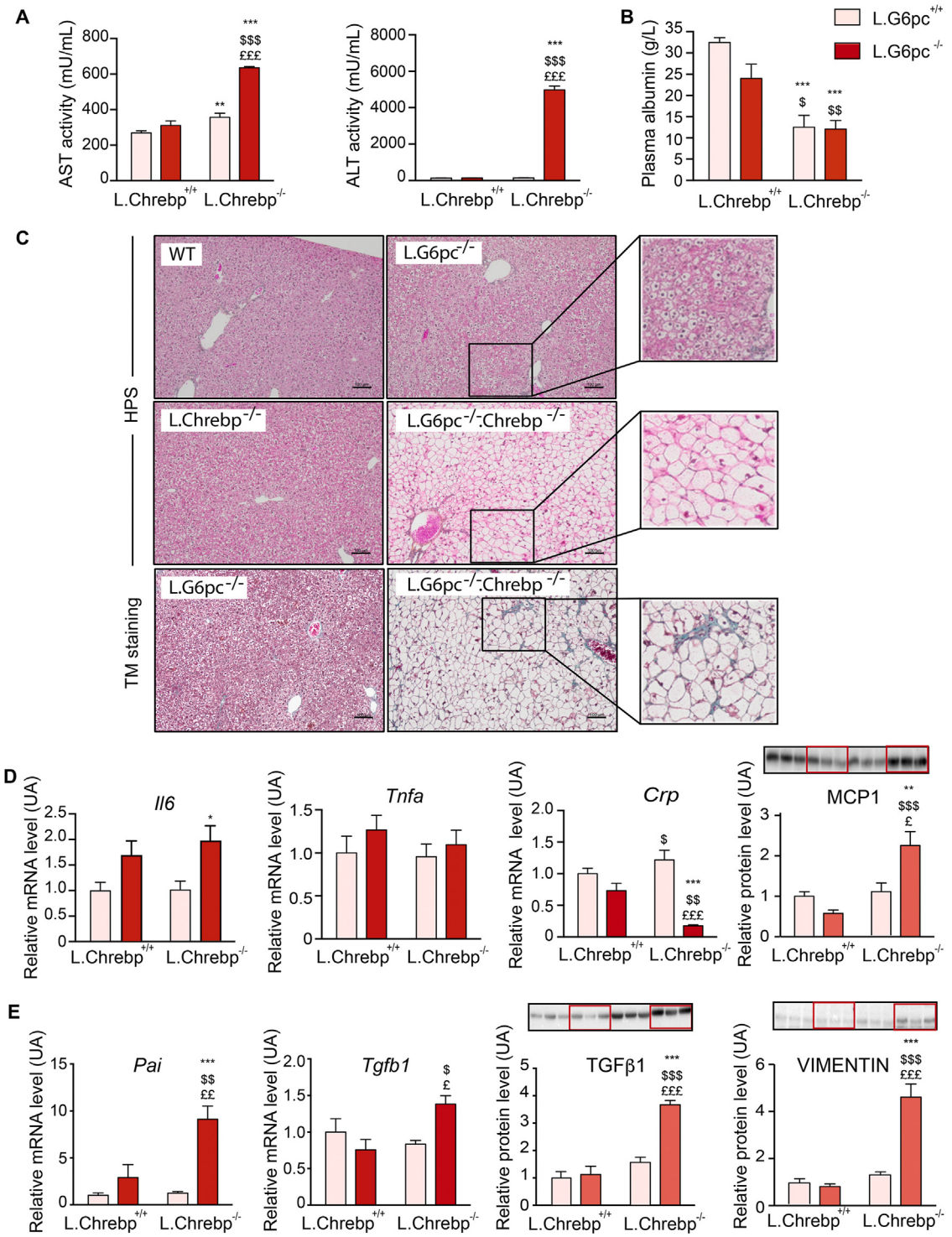

Figure 3: The loss of ChREBP in L.G6pc$^{-/-}$livers induces a severe liver phenotype. Control and L.Chrebp$^{-/-}$ mice (pink bars) and L.G6pc$^{-/-}$ and L.G6pc$^{-/-}$.Chrebp$^{-/-}$ mice (red bars) were fed a standard diet during 10 days after tamoxifen treatment. **(A)** Plasma concentrations of AST and ALT transaminases (n = 6–8/group). **(B)** Plasma concentration of albumin (n = 6–8/group). **(C)** Representative pictures of HPS staining and Trichrome's Masson (TM) staining of control (WT), L.G6pc$^{-/-}$, L.Chrebp$^{-/-}$ and L.G6pc$^{-/-}$.Chrebp$^{-/-}$ liver sections. Bars represent 100 μm. **(D–E)** Relative mRNA expression of *Il6* (coding for interleukin 6), *Tgfa*, *Crp, Pai* and *Tgfb1* (n = 6/group); western blot analyses of MCP1 (60 μg protein), TGFβ1 and vimentin (n = 6–8/group) in the livers. Representative images of western blots (n = 3) are shown above the quantification graph (n = 6–8/group). The quantification of western blots was performed relatively to the total amount of proteins using stained-free imaging technology (see Figure S5). Data are expressed as mean ± s.e.m. *p < 0.05, **p < 0.01 and ***p < 0.001 indicate significance compared to control mice; $^{\$}$p < 0.05, $^{\$\$}$p < 0.01, $^{\$\$\$}$p < 0.001 indicates significance compared to L.G6pc$^{-/-}$ mice; $^{£}$p < 0.05, $^{££}$p < 0.01 and $^{£££}$p < 0.001 indicate significance compared to L.Chrebp$^{-/-}$ mice. See also Figures S3 and S4.

knockout mice. In contrast, no difference in *Tnfa* (tumour necrosis factor α) expression was observed and or *Crp* (C reactive protein) mRNA level was even decreased. In addition, plasmatic MCP1 and TNFα levels were similar to control mice (Figure S4). Finally, mild fibrosis was observed in L.G6pc$^{-/-}$.Chrebp$^{-/-}$ livers, but not in L.G6pc$^{-/-}$ livers (Figure 3C). In agreement, an increase in *Pai* (encoding the plasminogen activator inhibitor-β1) and *Tgfb1* (encoding the transforming growth factor β1) gene expression was observed in double knockout livers compared to control or L.G6pc$^{-/-}$ livers (Figure 3E). The development of fibrosis in double knockout livers was also confirmed at the level of protein since the expression of TGFβ1 was increased in conjunction with sustained accumulation of extracellular matrix protein, such as vimentin (Figure 3E). However, inflammation and fibrosis were not further enhanced under HF diet challenge (Figure S3).

As previously observed in Chrebp$^{-/-}$ mice fed a high-fructose diet [22], the massive accumulation of glycogen caused important cellular stress related to an acute endoplasmic reticulum (ER) stress by activating the unfolded protein response (UPR) (Figure 4A). This was illustrated by a decrease of GRP78/BiP, associated with the accumulation of IRE1α and ATF4. In accordance with ATF4 overexpression, C/EBP homologous protein (CHOP) was specifically accumulated in L.G6pc$^{-/-}$.Chrebp$^{-/-}$ livers. Surprisingly, a decreased expression of cleaved pro-apoptotic proteins, i.e., cleaved caspase 3, caspase 7 and PARP, was observed in L.G6pc$^{-/-}$.Chrebp$^{-/-}$ livers (Figure 4B). Interestingly, the activation of ER stress was correlated to an induction in the expression of the fibroblast growth factor 21 (encoded by *fgf21*), resulting in an increase of FGF21 plasmatic levels (Figure 4C).

In conclusion, the combined loss of ChREBP and G6Pase in the liver causes severe stress to the hepatocytes by triggering high glycogen and water accumulation, leading in turn to acute liver injury. These results highlight the central role of ChREBP and G6Pase in maintaining hepatic homeostasis.

4. DISCUSSION

Disturbances in glucose and/or lipid homeostasis in the liver generally lead to the development of metabolic diseases characterised by NAFLD, as observed in type 2 diabetes or glycogen storage disease type I (GSDI), a rare metabolic disease due to the loss of G6Pase activity [23]. Of note, the early stage of NAFLD is characterised by the excessive accumulation of ectopic lipids in the liver and is often asymptomatic, without clinically relevant outcomes for decades. However, the histological lesions of NAFLD can progress to advanced fibrosis and even tumourigenesis. In this context, pharma industries develop numerous drugs targeting pathways directly or indirectly involved in the development of hepatic steatosis [24]. While ChREBP inhibition has been predicted to prevent hepatic steatosis, the current study highlights the essential role of the ChREBP/G6Pase couple and lipogenesis to maintain liver homeostasis by preventing glycogen-induced hepatomegaly.

Although it is now well known that ChREBP acts as a regulator of hepatic fatty acid synthesis and VLDL secretion, its deletion does not always lead to a decrease in lipid concentrations in the liver [13,25,26]. Thank to the L.G6pc$^{-/-}$ mouse model we developed, we report here the central metabolic role of ChREBP in the development of hepatic steatosis under conditions of G6P-dependent activation. In L.G6pc$^{-/-}$ liver, the blockade of G6Pase induces G6P accumulation, independently of carbohydrate intake. Accordingly, the impact of *Chrebp* inhibition was similar in L.G6pc$^{-/-}$ mice fed a standard or HF diet. Indeed, we observed a dramatic drop in TG content, with values below those measured in control livers and close to zero, under both nutritional conditions. We recently suggested that the normalisation of *Chrebp* mRNA levels in L.G6pc$^{-/-}$ liver using a shChrebp RNA inhibition strategy did not lead to a prevention of steatosis [27]. In contrast, an aggravation of NAFLD was observed in shChrebp-treated L.G6pc$^{-/-}$ liver due to a suppression of VLDL-TG export [27]. Although *Chrebp* silencing was associated with a decrease in *de novo* lipogenesis and of storage of newly synthesised lipids, steatosis was promoted by the accumulation of "old" fat in the shChrebp-treated L.G6pc$^{-/-}$ liver [27]. In agreement with previous data [13,28], our data here show that TG and cholesterol content was not modified in L.Chrebp$^{-/-}$ livers compared to control livers under standard or HF diets, despite a decrease in lipogenic gene expression. Thus, literature data and our results show the crucial role of ChREBP in the induction of lipogenesis exclusively in a G6P-dependent context. This is particularly relevant in metabolic diseases, such as GSDI or type 2 diabetes. It should be noted that in the case of diabetes, hyperinsulinaemia associated with hyperglycaemia enhances lipogenesis through the activation of sterol response element binding protein-1c (SREBP-1c), another key transcription factor that acts in synergy with ChREBP [29]. However, inhibition of ChREBP in the liver of obese and diabetic *ob/ob* mice results in decreased steatosis through the inhibition of the expression of lipogenic genes, without compensation by SREBP-1c [11,12]. Taken together, these data highlight the crucial role of ChREBP in controlling lipogenesis/esterification of fatty acids *via* the regulation of its activity by G6P.

The disruption of *Chrebp* also had an important impact on L.G6pc$^{-/-}$.Chrebp$^{-/-}$ whole body metabolism. Hepatic cholesterol content was decreased in liver of L.G6pc$^{-/-}$.Chrebp$^{-/-}$ mice fed a standard or HF diet compared with L.G6pc$^{-/-}$ mice but was similar to that in control mice. By contrast, cholesterol synthesis was not affected in shChrebp-treated L.G6pc$^{-/-}$ livers [27], while it was increased in high-fructose-fed Chrebp$^{-/-}$ mice [22], suggesting specific effects depending on the metabolic context. However, our data are in discrepancy with the conclusions of Zhang et al. [23], who suggested a key role of hepatic cholesterol accumulation in the development of liver damage in Chrebp$^{-/-}$ mice fed a high-fructose diet. Indeed, the same liver damages, associated with an UPR activation, were observed in L.G6pc$^{-/-}$.Chrebp$^{-/-}$ mice, while cholesterol content was not elevated. In the same study, it was also noted that ChREBP could block cholesterol biosynthesis via the destabilisation of SREBP2 protein under high-fructose diet condition [23]. By contrast, cholesterol biosynthesis was downregulated in the absence of ChREBP in L.G6pc$^{-/-}$.Chrebp$^{-/-}$ livers, *via* a decrease of *Srebp2* expression and, consequently, a decrease of *Hmgcs* and *Hmgcr* expression. It will therefore be necessary to further study the role of ChREBP in cholesterol biosynthesis in the liver. Finally, plasma TG and cholesterol levels were higher in L.G6pc$^{-/-}$.Chrebp$^{-/-}$ livers compared to L.G6pc$^{-/-}$ or control mice, despite the increase in CD36 expression. Hypertriglyceridaemia and hypercholesterolaemia were aggravated under HF diet conditions, suggesting that the impairment in hepatic lipid metabolism of L.G6pc$^{-/-}$.Chrebp$^{-/-}$ mice influenced their whole body lipid metabolism. The plasma accumulation of TG and cholesterol could be due to a lack of adipose tissue in the double knockout mice.

As mentioned above, G6P plays a crucial role in the induction of ChREBP activity and acts as a central hub for controlling hepatic metabolism by regulating glycogen storage, glycolysis, PPP, *de novo* lipogenesis and the hexosamine pathways [30]. Blocking one of these pathways in a healthy liver has generally limited consequences on liver homeostasis, whereas it can lead to metabolic imbalance in type 2 diabetes or GSDI. Our results strongly suggest that the loss of ChREBP leads to a decrease in glycolysis, PPP and *de novo* lipogenesis, and

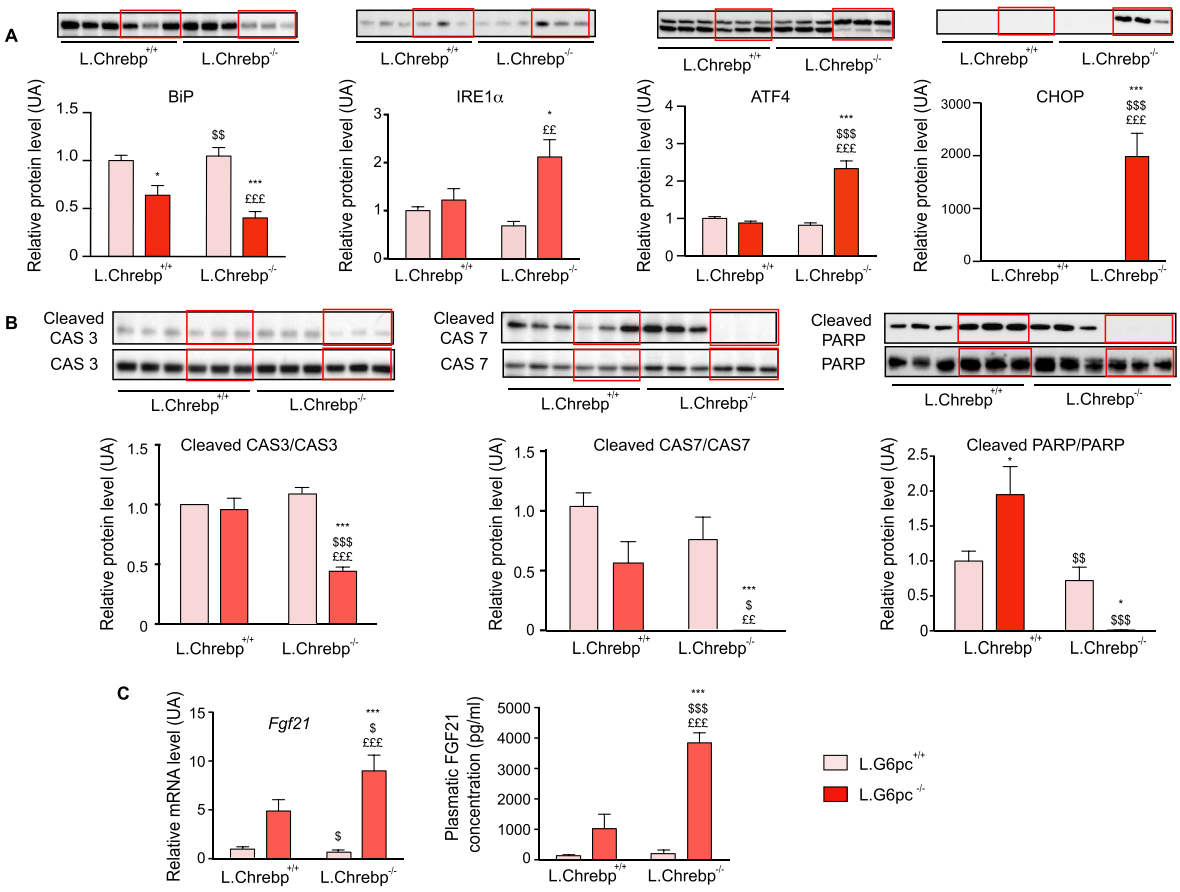

Figure 4: The loss of hepatic ChREBP in L.G6pc$^{-/-}$ mice induces hepatocyte cellular stress. Control and L.Chrebp$^{-/-}$ mice (pink bars) and L.G6pc$^{-/-}$ and L.G6pc$^{-/-}$.Chrebp$^{-/-}$ mice (red bars) were fed a standard diet during 10 days after tamoxifen treatment. Quantification of proteins involved **(A)** ER stress (BiP, Ire1α, ATF4 and CHOP) and **(B)** apoptosis (caspase 3, caspase 7 and PARP) by western blot analyses of protein extracts from the livers (n = 6–8/group). The quantification of proteins was performed relatively to the total amount of proteins using stained-free imaging technology (see Figure S5). For pro-apoptotic proteins, the cleaved protein quantity was expressed relatively to the total isoform. Representative images of western blots (n = 3) are shown above the quantification graphs (n = 6–8/group). **(C)** Relative mRNA expression of *Fgf21*in the liver (n = 4–6/group) and plasmatic FGF21 concentration (n = 6–8/group except for L.Chrebp$^{-/-}$ mice where n = 3). Data are expressed as mean ± s.e.m., relatively to control mice. *p < 0.05, **p < 0.01 and ***p < 0.001 indicates significance compared to control mice; $^{\$}$p < 0.05, $^{\$\$}$p < 0.01 and $^{\$\$\$}$p < 0.001 indicate significance compared to L.G6pc$^{-/-}$ mice; $^{£}$p < 0.05, $^{££}$p < 0.01 and $^{£££}$p < 0.001 indicate significance compared to L.Chrebp$^{-/-}$ mice.

that, as a consequence, G6P is routed towards glycogen synthesis. In agreement with this concept, glycogen content was higher in the livers of diabetic or *ob/ob* mice in the absence of ChREBP, as well as in shChrebp-treated L.G6pc$^{-/-}$ livers. In diabetic or *ob/ob* mice, ChREBP inhibition led to a decrease in *G6pc* expression, which resulted in a decrease of glucose production and an increase of glycogen synthesis [11,12]. Importantly, the combined loss of ChREBP and G6Pase in the livers led to massive hepatomegaly and ballooning hepatocytes that rapidly progressed to cell death, characterised by high levels of transaminases and associated with a discrete inflammation and mild fibrosis. In addition, glycogen overload associated with water retention induced important cell stress by acutely activating ER stress in L.G6pc$^{-/-}$.Chrebp$^{-/-}$ livers, as observed in Chrebp$^{-/-}$ mice under high-fructose diet [22]. In both cases, UPR activation, characterised by a decrease of the ER chaperone BiP/GRP78 and an increase of IRE1a, ATF6 and PERK/ATF4 pathways, was observed. Thus, the ATF4/CHOP was highly activated in L.G6pc$^{-/-}$.Chrebp$^{-/-}$ livers, which could be responsible for subsequent liver damage and then cell death [31]. Interestingly, it was previously reported that the acute depletion of CHOP could reverse liver injury in L.Chrebp$^{-/-}$ mice under high-fructose diet [22]. Moreover, it was recently shown that the PERK/ATF4 pathway is critical for ER stress-induced expression of FGF21, a hepatokine induced by various stresses, including glucose starvation, cold and autophagy deficiency [32]. Because ChREBP directly regulates *Fgf21* gene expression, in concert with PPARα [33,34], the deletion of ChREBP should blunt *Fgf21* transcription in L.G6pc$^{-/-}$.Chrebp$^{-/-}$ mice. It is interesting to note that FGF21 was overexpressed in the liver of double knockout mice, probably *via* the activation of ATF4/CHOP, suggesting that ChREBP is not mandatory for FGF21 expression. Finally, while the major death mechanism under chronic ER stress is apoptosis, markers of apoptosis were not induced in double knockout livers, suggesting the contribution of other types of cell death, possibly necrosis [31], to eliminate hepatocytes under osmotic imbalance due to the excess of water.

In conclusion, the initiation of lipid storage prevents cell damage driven by glycogen overload in the absence of G6Pase, which is likely due to over-activation of ChREBP by G6P or G6P derivatives. Indeed, liver ChREBP protects mice from fructose-induced hepatotoxicity by promoting *de novo* lipogenesis and regulating hepatic glycogen balance [35]. It was also recently proposed that a high ChREBP activation could

be an adaptive mechanism in Humans consuming large amounts of fructose to develop liver steatosis without severe liver injury [22]. Thus, the increase in *de novo* lipogenesis may be beneficial to maintain liver homeostasis under certain metabolic conditions.

5. CONCLUSION

Overall, maintaining homeostasis in hepatocytes is required to preserve liver function compatible with survival. The Anglo-Saxon etymology of the word liver, "lifere", is related to "life". Indeed, the liver was primarily seen as a vital organ, reflecting the exhibition of courage and of existence [36]; it was long believed that the liver was the source of blood and lymph. However, when this hypothesis was shown not to be true, the organ lost its attractiveness among physiologists. This stature was revived in the 19th century by the famous physiologist Claude Bernard, who highlighted many vital functions of the organ and discovered, in particular, the function of glucose production (he called this "glycogenesis") of the liver [37].
Our study emphasises the importance of maintaining G6P homeostasis in the liver, through the tight coordinate control exerted by ChREBP and G6Pase. This suggests that manipulating ChREBP or G6Pase as drug targets to preserve liver homeostasis in metabolic diseases could be potentially hazardous.

AUTHOR CONTRIBUTIONS

FR conceived and designed experiments, supervised the studies, analysed the data and wrote the paper; AC conducted experiments and analysed the data; MS conducted the *in vivo* experiments and monitored animal welfare; FL and MR were in charge of animal breeding; RD, AGS, CP and GM conceived experiments and critically edited the manuscript.

FINANCIAL SUPPORT STATEMENT

This work was supported by a research grant from the Agence Nationale de la Recherche, France (ANR-15-CE14-0026-03). Renaud Dentin is supported by the European Research Council (ERC-2013-StG-336629, LIPIDOLIV).

ACKNOWLEDGEMENTS

We would like to thank the members of Animalerie Lyon Est Conventionnelle et SPF (ALECS, SFR Santé Lyon-Est, Université Claude Bernard Lyon 1) for animal housing and care, and the members of the CiQLe platform for histological experiments (SFR Santé Lyon-Est, Université Claude Bernard Lyon 1). We thank Antonin Tortereau (PhD, Anatomical pathologist, Lyon) for histological analyses of the livers.

CONFLICT OF INTEREST

There is no conflict of interest to disclose relating to the work described in this paper.

APPENDIX A. SUPPLEMENTARY DATA

Supplementary data to this article can be found online at https://doi.org/10.1016/j.molmet.2020.101108.

REFERENCES

[1] Mithieux, G., Rajas, F., Gautier-Stein, A., 2004. A novel role for glucose 6-phosphatase in the small intestine in the control of glucose homeostasis. Journal of Biological Chemistry 279(43):44231–44234. https://doi.org/10.1074/jbc.R400011200.

[2] Mithieux, G., Rajas, F., Gautier-Stein, A., Soty, M., 2017. Adaptation of hepatic, renal and intestinal gluconeogenesis during food deprivation. In: Preedy, V., Patel, V.B. (Eds.), Handbook of famine, starvation, and nutrient deprivation. Springer International Publishing. p. 1–15.

[3] Soty, M., Gautier-Stein, A., Rajas, F., Mithieux, G., 2017. Gut-brain glucose signaling in energy homeostasis. Cell Metabolism 25(6):1231–1242. https://doi.org/10.1016/j.cmet.2017.04.032.

[4] Nordlie, R.C., Foster, J.D., Lange, A.J., 1999. Regulation of glucose production by the liver. Annual Review of Nutrition 19:379–406. https://doi.org/10.1146/annurev.nutr.19.1.379.

[5] Ponziani, F.R., Pecere, S., Gasbarrini, A., Ojetti, V., 2015. Physiology and pathophysiology of liver lipid metabolism. Expert Review of Gastroenterology & Hepatology 9(8):1055–1067. https://doi.org/10.1586/17474124.2015.1056156.

[6] Bechmann, L.P., Hannivoort, R.A., Gerken, G., Hotamisligil, G.S., Trauner, M., Canbay, A., 2012. The interaction of hepatic lipid and glucose metabolism in liver diseases. Journal of Hepatology 56(4):952–964. https://doi.org/10.1016/j.jhep.2011.08.025.

[7] Donnelly, K.L., Smith, C.I., Schwarzenberg, S.J., Jessurun, J., Boldt, M.D., Parks, E.J., 2005. Sources of fatty acids stored in liver and secreted via lipoproteins in patients with nonalcoholic fatty liver disease. Journal of Clinical Investigation 115(5):1343–1351. https://doi.org/10.1172/JCI23621.

[8] Postic, C., Girard, J., 2008. Contribution of de novo fatty acid synthesis to hepatic steatosis and insulin resistance: lessons from genetically engineered mice. Journal of Clinical Investigation 118(3):829–838. https://doi.org/10.1172/JCI34275.

[9] Ortega-Prieto, P., Postic, C., 2019. Carbohydrate sensing through the transcription factor ChREBP. Frontiers in Genetics 10:472. https://doi.org/10.3389/fgene.2019.00472.

[10] Abdul-Wahed, A., Guilmeau, S., Postic, C., 2017. Sweet sixteenth for ChREBP: established roles and future goals. Cell Metabolism 26(2):324–341. https://doi.org/10.1016/j.cmet.2017.07.004.

[11] Iizuka, K., Miller, B., Uyeda, K., 2006. Deficiency of carbohydrate-activated transcription factor ChREBP prevents obesity and improves plasma glucose control in leptin-deficient (ob/ob) mice. American Journal of Physiology. Endocrinology and Metabolism 291(2):E358–E364. https://doi.org/10.1152/ajpendo.00027.2006.

[12] Dentin, R., Benhamed, F., Hainault, I., Fauveau, V., Foufelle, F., Dyck, J.R.B., et al., 2006. Liver-specific inhibition of ChREBP improves hepatic steatosis and insulin resistance in ob/ob mice. Diabetes 55(8):2159–2170. https://doi.org/10.2337/db06-0200.

[13] Jois, T., Chen, W., Howard, V., Harvey, R., Youngs, K., Thalmann, C., et al., 2017. Deletion of hepatic carbohydrate response element binding protein (ChREBP) impairs glucose homeostasis and hepatic insulin sensitivity in mice. Molecular Metabolism 6(11):1381–1394. https://doi.org/10.1016/j.molmet.2017.07.006.

[14] Gjorgjieva, M., Calderaro, J., Monteillet, L., Silva, M., Raffin, M., Brevet, M., et al., 2018. Dietary exacerbation of metabolic stress leads to accelerated hepatic carcinogenesis in glycogen storage disease type Ia. Journal of Hepatology 69(5):1074–1087. https://doi.org/10.1016/j.jhep.2018.07.017.

[15] Mutel, E., Abdul-Wahed, A., Ramamonjisoa, N., Stefanutti, A., Houberdon, I., Cavassila, S., et al., 2011. Targeted deletion of liver glucose-6 phosphatase mimics glycogen storage disease type 1a including development of multiple adenomas. Journal of Hepatology 54(3):529–537. https://doi.org/10.1016/j.jhep.2010.08.014.

[16] Gjorgjieva, M., Oosterveer, M.H., Mithieux, G., Rajas, F., 2016. Mechanisms by which metabolic reprogramming in GSD1 liver generates a favorable tumorigenic environment. Journal of Inborn Errors of Metabolism and Screening 4:1–10. https://doi.org/10.1177/2326409816679429.

[17] Abdul-Wahed, A., Gautier-Stein, A., Casteras, S., Soty, M., Roussel, D., Romestaing, C., et al., 2014. A link between hepatic glucose production and peripheral energy metabolism via hepatokines. Molecular Metabolism 3(5): 531–543. https://doi.org/10.1016/j.molmet.2014.05.005.

[18] Monteillet, L., Gjorgjieva, M., Silva, M., Verzieux, V., Imikirene, L., Duchampt, A., et al., 2018. Intracellular lipids are an independent cause of liver injury and chronic kidney disease in non alcoholic fatty liver disease-like context. Molecular Metabolism 16:100–115. https://doi.org/10.1016/j.molmet.2018.07.006.

[19] Mithieux, G., Guignot, L., Bordet, J.-C., Wiernsperger, N., 2002. Intrahepatic mechanisms underlying the effect of metformin in decreasing basal glucose production in rats fed a high-fat diet. Diabetes 51(1):139–143.

[20] Colella, A.D., Chegenii, N., Tea, M.N., Gibbins, I.L., Williams, K.A., Chataway, T.K., 2012. Comparison of Stain-Free gels with traditional immunoblot loading control methodology. Analytical Biochemistry 430(2):108–110. https://doi.org/10.1016/j.ab.2012.08.015.

[21] Wilson, C.G., Tran, J.L., Erion, D.M., Vera, N.B., Febbraio, M., Weiss, E.J., 2016. Hepatocyte-specific disruption of CD36 attenuates fatty liver and improves insulin sensitivity in HFD-fed mice. Endocrinology 157(2):570–585. https://doi.org/10.1210/en.2015-1866.

[22] Zhang, D., Tong, X., VanDommelen, K., Gupta, N., Stamper, K., Brady, G.F., et al., 2017. Lipogenic transcription factor ChREBP mediates fructose-induced metabolic adaptations to prevent hepatotoxicity. Journal of Clinical Investigation 127(7):2855–2867. https://doi.org/10.1172/JCI89934.

[23] Rajas, F., Labrune, P., Mithieux, G., 2013. Glycogen storage disease type 1 and diabetes: learning by comparing and contrasting the two disorders. Diabetes & Metabolism 39(5):377–387. https://doi.org/10.1016/j.diabet.2013.03.002.

[24] Friedman, S.L., Neuschwander-Tetri, B.A., Rinella, M., Sanyal, A.J., 2018. Mechanisms of NAFLD development and therapeutic strategies. Nature Medicine 24(7):908–922. https://doi.org/10.1038/s41591-018-0104-9.

[25] Wu, W., Tsuchida, H., Kato, T., Niwa, H., Horikawa, Y., Takeda, J., et al., 2015. Fat and carbohydrate in western diet contribute differently to hepatic lipid accumulation. Biochemical and Biophysical Research Communications 461(4): 681–686. https://doi.org/10.1016/j.bbrc.2015.04.092.

[26] Erion, D.M., Popov, V., Hsiao, J.J., Vatner, D., Mitchell, K., Yonemitsu, S., et al., 2013. The role of the carbohydrate response element-binding protein in male fructose-fed rats. Endocrinology 154(1):36–44. https://doi.org/10.1210/en.2012-1725.

[27] Lei, Y., Hoogerland, J.A., Bloks, V.W., Bos, T., Bleeker, A., Wolters, H., et al., 2020. Hepatic ChREBP activation limits NAFLD development in a mouse model for Glycogen Storage Disease type Ia. Hepatology: hep. 31198. https://doi.org/10.1002/hep.31198.

[28] Niwa, H., Iizuka, K., Kato, T., Wu, W., Tsuchida, H., Takao, K., et al., 2018. ChREBP rather than SHP regulates hepatic VLDL secretion. Nutrients 10(3). https://doi.org/10.3390/nu10030321.

[29] Wang, Y., Viscarra, J., Kim, S.-J., Sul, H.S., 2015. Transcriptional regulation of hepatic lipogenesis. Nature Reviews Molecular Cell Biology 16(11):678–689. https://doi.org/10.1038/nrm4074.

[30] Rajas, F., Gautier-Stein, A., Mithieux, G., 2019. Glucose-6 phosphate, A central hub for liver carbohydrate metabolism. Metabolites 9(12). https://doi.org/10.3390/metabo9120282.

[31] Urra, H., Dufey, E., Lisbona, F., Rojas-Rivera, D., Hetz, C., 2013. When ER stress reaches a dead end. Biochimica et Biophysica Acta (BBA) - Molecular Cell Research 1833(12):3507–3517. https://doi.org/10.1016/j.bbamcr.2013.07.024.

[32] Kim, S.H., Kim, K.H., Kim, H.-K., Kim, M.-J., Back, S.H., Konishi, M., et al., 2015. Fibroblast growth factor 21 participates in adaptation to endoplasmic reticulum stress and attenuates obesity-induced hepatic metabolic stress. Diabetologia 58(4):809–818. https://doi.org/10.1007/s00125-014-3475-6.

[33] Iroz, A., Montagner, A., Benhamed, F., Levavasseur, F., Polizzi, A., Anthony, E., et al., 2017. A specific ChREBP and PPARα cross-talk is required for the glucose-mediated FGF21 response. Cell Reports 21(2):403–416. https://doi.org/10.1016/j.celrep.2017.09.065.

[34] Montagner, A., Polizzi, A., Fouché, E., Ducheix, S., Lippi, Y., Lasserre, F., et al., 2016. Liver PPARα is crucial for whole-body fatty acid homeostasis and is protective against NAFLD. Gut: gutjnl 2015:310798. https://doi.org/10.1136/gutjnl-2015-310798.

[35] Shi, J.-H., Lu, J.-Y., Chen, H.-Y., Wei, C.-C., Xu, X., Li, H., et al., 2020. Liver ChREBP protects against fructose-induced glycogenic hepatotoxicity by regulating L-type pyruvate kinase. Diabetes 69(4):591–602. https://doi.org/10.2337/db19-0388.

[36] Riva, M.A., Riva, E., Spicci, M., Strazzabosco, M., Giovannini, M., Cesana, G., 2011. "The city of Hepar": rituals, gastronomy, and politics at the origins of the modern names for the liver. Journal of Hepatology 55(5):1132–1136. https://doi.org/10.1016/j.jhep.2011.05.011.

[37] Bernard, C., 1853. Nouvelle fonction du foie considéré comme organe producteur de matière sucrée chez l'homme et les animaux. Paris: Baillière JB.

